



## **Phosphatase Wip1 Is Essential for the Maturation and Homeostasis of Medullary Thymic Epithelial Cells in Mice**

This information is current as  
of November 3, 2013.

Lina Sun, Hongran Li, Haiying Luo, Lianjun Zhang, Xuelian  
Hu, Tao Yang, Chenming Sun, Hui Chen, Lianfeng Zhang  
and Yong Zhao

*J Immunol* 2013; 191:3210-3220; Prepublished online 21  
August 2013;  
doi: 10.4049/jimmunol.1300363  
<http://www.jimmunol.org/content/191/6/3210>

**Supplementary  
Material** <http://www.jimmunol.org/content/suppl/2013/08/21/jimmunol.1300363.DC1.html>

**References** This article **cites 45 articles**, 19 of which you can access for free at:  
<http://www.jimmunol.org/content/191/6/3210.full#ref-list-1>

**Subscriptions** Information about subscribing to *The Journal of Immunology* is online at:  
<http://jimmunol.org/subscriptions>

**Permissions** Submit copyright permission requests at:  
<http://www.aai.org/ji/copyright.html>

**Email Alerts** Receive free email-alerts when new articles cite this article. Sign up at:  
<http://jimmunol.org/cgi/alerts/etoc>

# Phosphatase Wip1 Is Essential for the Maturation and Homeostasis of Medullary Thymic Epithelial Cells in Mice

Lina Sun,<sup>\*,1</sup> Hongran Li,<sup>\*,1</sup> Haiying Luo,<sup>\*</sup> Lianjun Zhang,<sup>\*</sup> Xuelian Hu,<sup>\*</sup> Tao Yang,<sup>\*</sup> Chenming Sun,<sup>\*</sup> Hui Chen,<sup>\*</sup> Lianfeng Zhang,<sup>†</sup> and Yong Zhao<sup>\*</sup>

Thymic epithelial cells (TECs) are a key cell type in the thymic microenvironment essential for T cell development. However, intrinsic molecular mechanisms controlling TEC differentiation and activities are poorly defined. In this study, we found that deficiency of p53-induced phosphatase 1 (Wip1) in mice selectively caused severe medullary TEC (mTEC) maturation defects in an intrinsic manner. Wip1 knockout (KO) mice had decreased mature epithelial cell adhesion molecule<sup>+</sup>*Ulex europaeus* agglutinin-1 (UEA-1)<sup>+</sup> mTECs, including UEA-1<sup>+</sup>MHC class II<sup>high</sup>, UEA-1<sup>+</sup>CD80<sup>+</sup>, UEA-1<sup>+</sup>CD40<sup>+</sup>, and UEA-1<sup>+</sup>Aire<sup>+</sup> cells, but not decreased numbers of cortical epithelial cell adhesion molecule<sup>+</sup>BP-1<sup>+</sup> TECs, in the postnatal stage but not in the fetal stage. Wip1-deficient mTECs express fewer tissue-restricted Ags and UEA-1<sup>+</sup>involucrin<sup>+</sup> terminal-differentiated cells. Animal models, including grafting fetal Wip1-deficient thymic tissue into T cell-deficient nude mice and reconstitution of lethally irradiated Wip1KO mouse recipients with wild-type bone marrow cells, also showed the impaired mTEC components in Wip1KO thymi, indicating the intrinsic regulatory role of Wip1 in mTEC maturation. Furthermore, thymus regeneration was significantly less efficient in adult Wip1KO mice than in wild-type mice after cyclophosphamide treatment. Wip1 deficiency resulted in elevated p38 MAPK activity in mTECs. Activated p38 MAPK has the ability to suppress CD40 expression on mTECs. Wip1-deficient thymi displayed poor response to CD40L in the fetal thymus organ culture system. Thus, Wip1 positively controls mTEC maturation, homeostasis, and regeneration through limiting the p38 MAPK pathway. *The Journal of Immunology*, 2013, 191: 3210–3220.

The thymus, as a primary lymphoid organ, is critical for T cell development and maturation. Among all thymic cell components, thymic epithelial cells (TECs) are of the most significance to provide a highly specialized microenvironment for the functional and self-tolerant T cell maturation from lymphoid progenitor cells in the thymus (1). Based on the localization in thymus and distinctive cell surface markers, TECs are roughly divided into two major subsets, cortical TECs (cTECs) and medullary TECs (mTEC) (2). These two morphologically and functionally distinct types of TECs arise from a common bipotent progenitor cell under a complex regulatory network (3, 4). Foxn1 is a transcription factor that plays a central role in TEC differentiation and is required at multiple intermediate stages of TEC lineage development in both the fetal and adult thymus (5, 6). TNFR superfamily (TNFRSF) members, including receptor activator for NF- $\kappa$ B (RANK), CD40, and lymphotoxin  $\beta$  (LT $\beta$ ) receptor, are important for the development of mTECs via NF- $\kappa$ B activation (7–10). However, the precise developmental pathways

and molecular mechanisms regulating TEC maturation remain poorly defined. Understanding the processes that control TEC commitment, differentiation, and survival/turnover is still a major challenge for our current thymus research.

Wild-type (WT) p53-induced phosphatase 1 (Wip1, also called PP2C $\delta$ ), which is encoded by protein phosphatase magnesium-dependent 1 $\delta$ , is a serine/threonine protein phosphatase belonging to the type 2C $\delta$  protein phosphatases (11). It is activated by various stresses and is involved in various cellular processes, including tumorigenesis and aging (reviewed in Refs. 12, 13). Wip1 is recognized as a novel oncogene and inhibits several p53-dependent tumor suppressor pathways, for example, the ATM/CHK2/p53 and p38 MAPK/p53 pathways, as well as the NF- $\kappa$ B pathway (14–17). It was reported that smaller thymus and impaired thymocyte development were observed in Wip1 knockout (KO) mice (18). However, the direct effects of Wip1 on TEC development have not been addressed. In this study, we employed Wip1KO mice and various mouse models to investigate the role of

<sup>\*</sup>State Key Laboratory of Biomembrane and Membrane Biotechnology, Institute of Zoology, Chinese Academy of Sciences, Beijing, China 100101; and <sup>†</sup>Key Laboratory of Human Diseases Comparative Medicine, Ministry of Health, Institute of Laboratory Animal Science, Chinese Academy of Medical Sciences and Peking Union Medical College, Beijing, China 100021

<sup>1</sup>L.S. and H. Li contributed equally to this work as cofirst authors.

Received for publication February 6, 2013. Accepted for publication July 22, 2013.

This work was supported by National Basic Research Program of China Grants 2010CB945301 and 2011CB710903 (to Y.Z.), National Natural Science Foundation for General and Key Programs Grants C81130055, C81072396 (to Y.Z.), and C31200681 (to H. Luo), and Knowledge Innovation Program of Chinese Academy of Sciences Grant YSCX2-YW-238 (to Y.Z.).

L.S. designed and performed the experiments with cells and mice, analyzed data, and contributed to writing the manuscript; H. Li designed and performed the experiments, analyzed histology data, and contributed to managing the mouse colonies; H. Luo performed flow cytometry; L. Zhang performed TEC isolation; X.H. performed flow cytometry and mouse breeding; T.Y. performed the cell signal assays; C.S. performed the CD40 expression assays; H.C. performed real-time PCR assays; L. Zhang provided animal models and revised the manuscript; and

Y.Z. designed experiments, analyzed data, wrote the manuscript, and provided overall direction.

Address correspondence and reprint requests to Dr. Yong Zhao or Dr. Lianfeng Zhang, Transplantation Biology Research Division, State Key Laboratory of Biomembrane and Membrane Biotechnology, Institute of Zoology, Chinese Academy of Sciences, Beichen Western Road 1-5, Chaoyang District, Beijing, China 100101 (Y.Z.) or Key Laboratory of Human Diseases Comparative Medicine, Ministry of Health, Institute of Laboratory Animal Science, Chinese Academy of Medical Sciences and Peking Union Medical College, Chao Yang Strict, Pan Jia Yuan Nan Li No. 5, Beijing, China 100021 (L.Z.). E-mail addresses: zhaoy@ioz.ac.cn (Y.Z.) or zhanglf@cnilas.org (L.Z.)

The online version of this article contains supplemental material.

Abbreviations used in this article: BMC, bone marrow cell; CK, cytokeratin; cTEC, cortical thymic epithelial cell; Cy, cyclophosphamide; EpCAM, epithelial cell adhesion molecule; FGF, fibroblast growth factor; FTOC, fetal thymus organ culture; KO, knockout; LT $\beta$ , lymphotoxin  $\beta$ ; MHC II, MHC class II; mTEC, medullary thymic epithelial cell; RANK, receptor activator for NF- $\kappa$ B; TEC, thymic epithelial cell; TNFRSF, TNFR superfamily; UEA-1, *Ulex europaeus* agglutinin-1; WT, wild-type.

Copyright © 2013 by The American Association of Immunologists, Inc. 0022-1767/13/\$16.00

Wip1 in TEC development, homeostasis, and function. Our results showed that Wip1 significantly regulated mTEC but not cTEC maturation and homeostasis in a cell-intrinsic and positive manner.

## Materials and Methods

### Mice

Wip1KO mice and GFP-transgenic mice were provided by the Key Laboratory of Human Diseases Comparative Medicine, Ministry of Public Health (Beijing, China). Wip1KO mice have been described previously (15, 19) and were backcrossed to the C57BL/6 genetic background in our laboratory (20). BALB/c nude mice were purchased from Beijing University Experimental Animal Center (Beijing, China). All mice were bred and maintained in specific pathogen-free conditions. Sex-matched littermate mice 4–6 wk of age were mainly used for experiments. All animal experiments were performed in accordance with the approval of the Animal Ethics Committee of the Institute of Zoology, Beijing, China.

### Abs and flow cytometry

The following biotinylated or fluorochrome-conjugated Abs were used in flow cytometry detection. Biotinylated *Ulex europaeus* agglutinin-1 (UEA-1) was obtained from Vector Laboratories and revealed with streptavidin-PE (BD Pharmingen) or Alexa Fluor 610-R-PE (Invitrogen). Anti-CD4-FITC and anti-CD8-PE were from Tianjin Sungen Biotech (Tianjin, China). Anti-BP-1-PE (Ly51, clone 6C3) was from eBioscience. The following Abs were purchased from BioLegend: anti-CD45-PerCP/Cy5.5 or -PE/Cy5 (clone 30-F11), anti-epithelial cell adhesion molecule (EPCAM)-FITC or -PE or -PE/Cy7 (clone G8.8), anti-I-Ab-PE (clone AF6-120.1), Alexa Fluor 488 anti-I-A/I-E (clone M5/114.15.2), anti-CD80-PE (clone 16-10A1), anti-CD40-PE (clone 3/23), anti-CD8-PE/Cy5 (clone 53-6.7), anti-RANK-PE (clone R12-31), and anti-LT $\beta$ R-PE (clone 5G11). Anti-MTS24 Ab was offered by Prof. Richard Boyd (Monash University). Surface staining of cell suspensions was performed in PBS/0.1% BSA/0.02% Na<sub>2</sub>S<sub>2</sub>O<sub>3</sub> solution at 4°C. For flow cytometric analysis of phosphorylated p38 MAPK, Alexa Fluor 488 anti-p38 MAPK (pT180/pY182) was purchased from BD Pharmingen and performed according to the manufacturer's protocol. Intracellular staining for Foxp3-PE (eBioscience), Aire-FITC (provided by Prof. Francois-Xavier Hubert, Walter and Eliza Hall Institute of Medical Research), or Aire-Alexa Fluor 647 (clone 5H12; eBioscience) and Ki-67 (BD Pharmingen) were performed using fixation buffer (eBioscience) and permeabilization buffer (eBioscience) according to the manufacturers' protocols. Apoptosis of TECs was quantified by an *in situ* cell death detection kit (Roche) by flow cytometry following the manufacturer's instructions.

### Immunohistology and immunofluorescence

For analysis of thymic medulla and cortex by immunohistology, thymi from Wip1KO mice and age-matched WT control mice were fixed in 4% formalin and embedded in paraffin blocks. Sections (5  $\mu$ m) were stained with H&E and examined by light microscopy. For immunofluorescence, serial sections (5  $\mu$ m) from OCT-embedded frozen tissues were fixed in cold acetone and blocked in PBS/1% BSA, washed in PBS/0.05% Tween 20, and incubated with optimal dilutions of anti-cytokeratin 5 (Abcam) and anti-cytokeratin 8 (Troma-I; Developmental Studies Hybridoma Bank, Iowa City, IA), biotinylated UEA-1, and Alexa Fluor 488 anti-I-A/I-E for 2 h at room temperature before washing and incubating with secondary reagents, that is, Alexa Fluor 546 goat anti-rabbit IgG (H+L), Alexa Fluor 488 goat anti-rat IgG (H+L) (Invitrogen), and streptavidin-PE. Control slides were incubated with isotype-matched Ig. Images were acquired with two-photon microscopy (Carl Zeiss). For calculating thymic area, images from immunofluorescence and H&E staining were captured with the CRI Nuance v2.8 multispectral imaging system (Cambridge Research and Instrumentation, Woburn, MA). The resulting images were mathematically unmixed into individual cytokeratin (CK)5 substrate, CK8 substrate using spectra deduced from control specimens to remove nonspecific fluorescence. In-Form v1.2 software (CRI) was used to calculate area size and ratio.

### Thymic stromal cell isolation and *in vitro* culture of TECs

Thymic stromal cells from postnatal thymi were isolated as previously described (21). In brief, freshly dissected thymi were cut into 1-mm<sup>3</sup> pieces and washed with DMEM medium with 2% FBS several times to remove most thymocytes. The thymic fragments were then incubated at 37°C for 10 min in 2 ml solution of 1 mg/ml collagenase D (equivalent to 0.1% [w/v]) with 20 U/ml DNase I (Sigma-Aldrich). Enzymatic treatment was repeated three times (the final incubation with collagenase/dispase enzyme mixture) until all fragments were dispersed. Gentle agitation was performed peri-

odically at mid- and endpoints of each digestion. Cell suspensions from each digestion were pooled in PBS containing 1% FBS and 5 mM EDTA to neutralize digestion and remove cell aggregates. Cells were centrifuged, resuspended in DMEM with 2% FBS medium, and filtered to remove clumps. Phenotypes of TECs were analyzed by surface FACS staining.

For TEC culture, thymi from WT neonatal mice were digested as mentioned above. Small thymic fragments from each step were collected and pooled. Fragments were allowed to settle and washed twice with PCT medium (CnT07; CELLnTEC). The remaining thymic explants were plated in 48-well plates with CnT07 medium and cultured at 37°C and 5% CO<sub>2</sub> for several days, during which TECs outgrew other stromal cells. To determine the effect of p38 MAPK and STAT1 signaling on the expression of CD40, cultured TECs were treated with 50  $\mu$ M p38 MAPK inhibitor (SB203580; Sigma-Aldrich) or 400  $\mu$ M STAT1 inhibitor (MTA; Sigma-Aldrich). After 48 h of treatment, TECs were collected with trypsin (Sigma-Aldrich) digestion and analyzed for CD40 expression by FACS.

### Fetal thymus organ culture

Fetal thymus organ culture (FTOC) was performed as described previously (7). Briefly, thymic lobes were isolated from embryos 16.5 d after coitus and were cultured for 4 d on the top of Nuclepore filters (Whatman) placed in DMEM medium supplemented with 10% FBS (Life Technologies), 2 mM L-glutamine, 100 U/ml penicillin, 100 mg/ml streptomycin, and 50 mM 2-ME containing 1.35 mM 2'-deoxyguanosine (Sigma-Aldrich). To test the mTEC differentiation using FTOC, 2'-deoxyguanosine-treated fetal thymic lobes were cultured in DMEM plus 10% FBS with recombinant CD40L (2.5  $\mu$ g/ml; PeproTech) or RANKL (1  $\mu$ g/ml; Sigma-Aldrich). Four days after stimulation, the lobes were harvested for flow cytometric analysis.

### BrdU incorporation assays

For BrdU (BD Biosciences) labeling, 4-wk-old Wip1KO and WT mice were injected with 1 mg/day BrdU in PBS *i.p.* for 2 consecutive days. Twenty-four hours after the secondary injection, thymic lobes were digested, and thymic stromal cells were enriched for flow cytometric analysis as mentioned above. BrdU incorporation was detected with a FITC-BrdU flow kit (BD Biosciences) according to the manufacturer's protocol.

### Cyclophosphamide treatment

Mice were injected *i.p.* with cyclophosphamide (Cy) at a dose of 100 mg/kg body weight per day for 2 consecutive days. The first day after Cy treatment was considered to be recovery day 1.

### Quantitative RT-PCR

RNA was purified from WT and Wip1KO mTECs sorted by flow cytometry and characterized as CD45<sup>+</sup>EPCAM<sup>+</sup>UEA-1<sup>+</sup>. mRNA was prepared using an RNeasy Mini kit (Qiagen) and the cDNA library was generated with a reverse transcription system kit (Promega) according to the manufacturers' protocols. Quantitative PCR was performed using SYBR Premix Ex Taq (TaKaRa Bio). Relative expression values for target genes normalized to HPRT were obtained. The primers used in the current study were listed in Table 1.

### Bone marrow chimeras and fetal thymus transplantation models

Bone marrow cells (BMCs) from 12-wk-old B6-GFP mice were prepared. BMCs ( $1 \times 10^7$ ) were injected into the tail vein of lethally irradiated 6- to 8-wk-old WT and Wip1KO recipients to set up full chimeras as described (22, 23). Mice were sacrificed 8 wk after reconstitution, and the percentages of donor-derived cells were revealed as GFP<sup>+</sup> by flow cytometry.

Thymic lobes from E16.5 Wip1KO and WT embryos were used for transplantation. Thymic lobes were surgically transplanted under the kidney capsule of adult nude recipients (24). Mice were sacrificed after 6 wk transplantation. Grafts of thymus were harvested and analyzed for TEC phenotype.

### Statistical analysis

All data are presented as the means  $\pm$  SD. A Student unpaired *t* test for comparison of means was used to compare groups. A *p* value of <0.05 was considered statistically significant.

## Results

### Wip1 deficiency selectively impairs mTEC maturation

Wip1KO mice, in which Wip1 expression was eliminated via gene targeting as reported previously (15), were bred back to have a B6

genetic background (20). These Wip1KO mice were fertile and displayed no gross abnormalities within 3 mo after birth. However, Wip1KO mice had a thymus defect as evidenced by the small thymus size, the low ratio of thymus weight to body weight, and decreased cell number of thymocytes compared with age-matched WT mice ( $p < 0.01$ , Fig. 1A–C), which is consistent with the previous report (18). To assess the effect of Wip1 deficiency on TECs, we analyzed the levels of CD45<sup>+</sup>EpCAM<sup>+</sup> TECs of Wip1KO and WT mice using FACS. The percentage and cell number of CD45<sup>+</sup>EpCAM<sup>+</sup> TECs in the thymi of Wip1KO mice were significantly lower than those in WT mice ( $p < 0.001$ , Fig. 1D–F). In addition to the decreased thymic size and cell number, thymi of Wip1-deficient mice had significantly smaller medulla compared with WT mice, as shown in the thymic sections stained with H&E or stained with mAbs against CK5 and CK8 ( $p < 0.001$ , Fig. 1G–K). Decreased CK5/MHC class II (MHC II)<sup>+</sup> and UEA-1/MHC II<sup>+</sup> positive areas were also observed in Wip1KO mice compared with WT mice (data not shown).

mTECs display terminal L-fucosyl residues that bind to plant lectin UEA-1 (25). Thus, UEA-1 was used as a surface marker to define the mTEC subpopulation, in addition to intracellular expression of CK5 (6, 9). Functional maturation of UEA-1<sup>+</sup> mTECs is marked by upregulation of MHC II, CD80, and CD40 molecules as well as the transcriptional regulator Aire (26–30). After observing the decreased medullary-to-cortical area ratio in Wip1KO mice, we investigated the mTEC phenotypes in these mice. As shown in Fig. 2, the percentage and cell number of UEA-1<sup>+</sup> mTECs were significantly decreased in Wip1KO mice ( $p < 0.001$ , Fig. 2A–C). More impressively, the presence of maturing EpCAM<sup>+</sup>UEA-1<sup>+</sup> mTECs, including MHC II<sup>high</sup>, CD80<sup>+</sup>, CD40<sup>+</sup>,

and Aire<sup>+</sup> cells, was markedly decreased in Wip1KO mice ( $p < 0.001$ , Fig. 2D–F). In line with the impaired maturation phenotypes of mTECs, the expressions of Aire-dependent and -independent tissue-restricted Ags, such as spt1, insulin 2, Tff3, Mup1, nAchr-1, GAD67, and CRP in sorted Wip1-deficient mTECs, were significantly decreased as determined by real-time PCR assays (Fig. 2G, Table I). It has been reported that mTECs might further differentiate into terminally differentiated involucrin<sup>+</sup> mTECs and form Hassall's corpuscles (31). Indeed, Wip1KO mice had defective Hassall's corpuscles as determined by H&E staining (Fig. 2H) and a significantly decreased cell number of involucrin<sup>+</sup>UEA-1<sup>+</sup> mTECs in the thymus as assayed by flow cytometry ( $p < 0.001$ , Fig. 2I). Thus, Wip1 deficiency caused a defect of mTEC maturation in mice.

In contrast to mTECs, the total cell numbers of cTECs including EpCAM<sup>+</sup>BP-1<sup>+</sup> and EpCAM<sup>+</sup>BP-1<sup>+</sup>CD40<sup>+</sup> cells were indistinguishable in Wip1KO mice compared with WT mice ( $p > 0.05$ , Fig. 3A, 3B). The percentage of EpCAM<sup>+</sup>BP-1<sup>+</sup> cells in EpCAM<sup>+</sup> cells was increased in Wip1KO mice compared with WT mice (Fig. 3A), possibly due to the decreased mTEC components ( $p < 0.001$ , Fig. 2B). Thus, Wip1 deficiency selectively affects the development and maturation of EpCAM<sup>+</sup>UEA-1<sup>+</sup> mTECs in the thymus.

The distribution of thymocyte subsets, including CD4<sup>+</sup>CD8<sup>−</sup>, CD4<sup>+</sup>CD8<sup>+</sup>, CD4<sup>−</sup>CD8<sup>−</sup>, and CD4<sup>−</sup>CD8<sup>+</sup> thymocytes, was altered in Wip1KO mice ( $p < 0.05$ , Fig. 3C) as reported previously (18). The total cell numbers of these thymocyte subsets were decreased in Wip1KO mice ( $p < 0.001$ , Fig. 3C), mainly due to the dramatic decrease of the total cell number of thymocytes (Fig. 1C). These changes also indirectly support the functional alter-

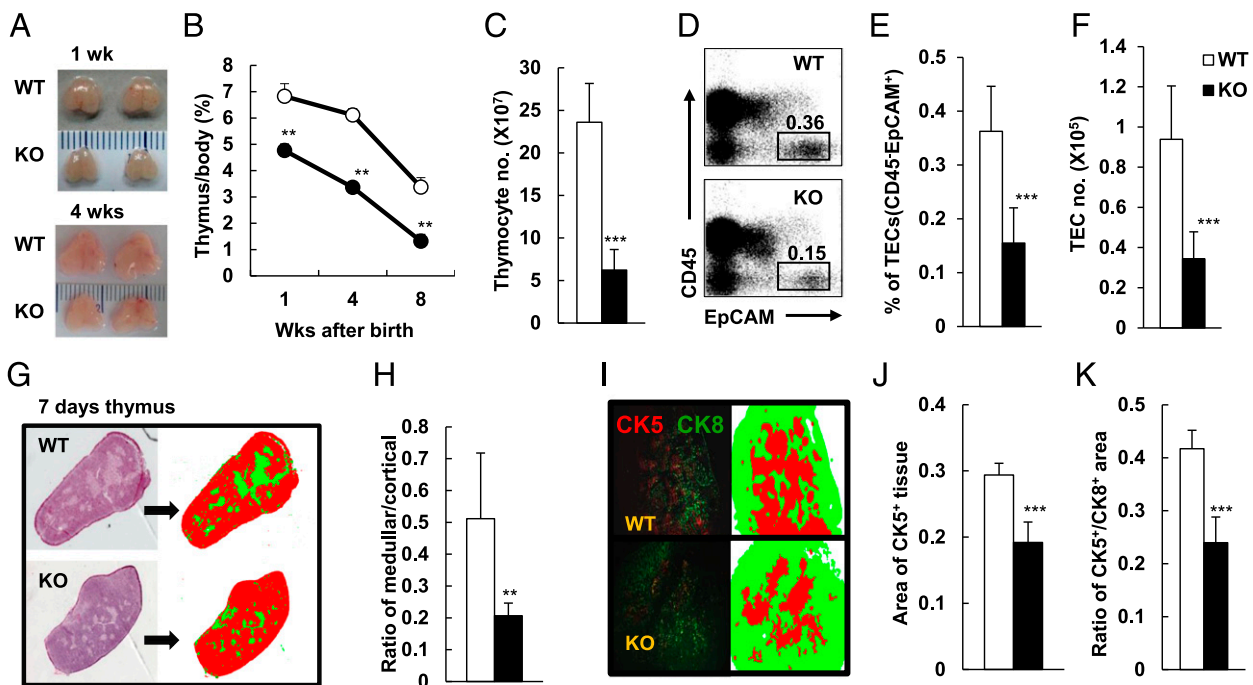


**FIGURE 1.** Selectively decreased thymic medullary region was detected in Wip1KO mice. (A) Representative photographs of thymus organs in WT and Wip1KO mice is shown. (B) Ratios of thymus weight to body weight in Wip1KO mice (●) were significantly lower than in WT mice (○). (C) Total cell numbers of thymocytes in WT (open bar) and Wip1KO (filled bar) mice are presented. (D) Representative FACS analysis of CD45<sup>+</sup>EpCAM<sup>+</sup> TECs in the isolated thymic cells is shown. The percentage (E) and the total cell number (F) of CD45<sup>+</sup>EpCAM<sup>+</sup> TECs in WT and Wip1KO mice are shown. (G) H&E staining of the thymus of 7-d-old WT and Wip1KO mice is shown. (H) The ratio of thymic medullary region to cortical region in 7-d-old Wip1KO mice was less than in WT mice. (I) The CK5/CK8 staining of the thymus of 7-d-old WT and Wip1KO mice is presented. (J) The area of thymic medullary region in 7-d-old Wip1KO mice is smaller than in WT mice. (K) The ratio of CK5/CK8 area in the thymus of 7-d-old Wip1KO mice was less than in WT mice. Data presented are means  $\pm$  SD ( $n = 6$ ). Representative results are shown from one of three independent experiments performed. \*\* $p < 0.01$ , \*\*\* $p < 0.001$  (WT versus Wip1KO mice).

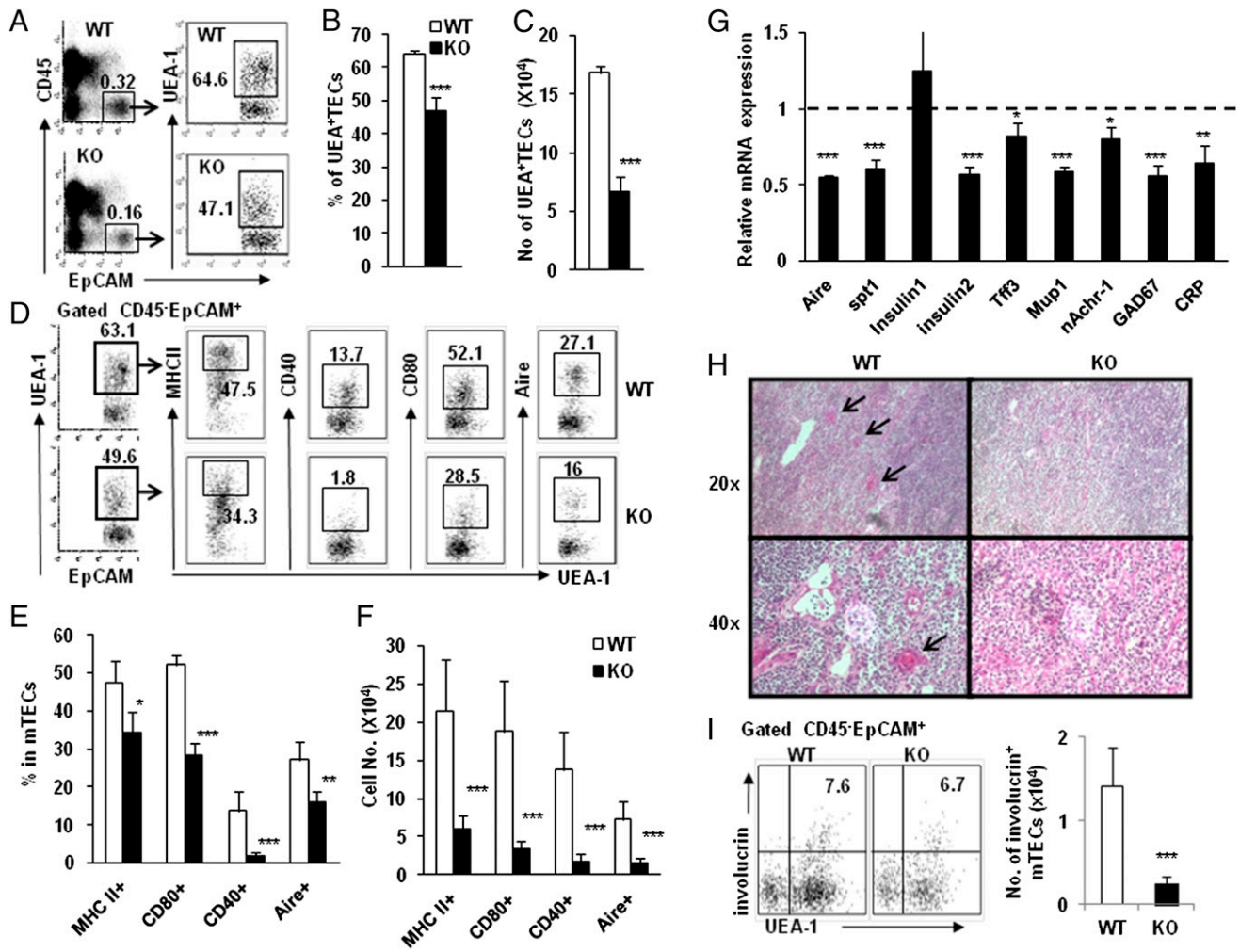


**FIGURE 2.** Mature mTECs were significantly decreased in Wip1-deficient mice. (A) FACS analysis of CD45<sup>-</sup>EpCAM<sup>+</sup> UEA-1<sup>+</sup> cells of 8-wk-old WT and Wip1KO mice. (B) Percentage of UEA-1<sup>+</sup> cells among the gated CD45<sup>-</sup>EpCAM<sup>+</sup> cells in WT and Wip1KO mice. (C) The cell number of CD45<sup>-</sup>EpCAM<sup>+</sup> UEA-1<sup>+</sup> cells in the thymus of WT and Wip1KO mice is shown (mean ± SD, n = 7 mice of each genotype). (D) Phenotypic characterization of MHC II, CD40, CD80, and Aire expressions in the gated thymic CD45<sup>-</sup>EpCAM<sup>+</sup> UEA-1<sup>+</sup> cells of WT and Wip1KO mice. (E) Frequencies of MHC II<sup>high</sup>, CD80<sup>+</sup>, CD40<sup>+</sup>, and Aire<sup>+</sup> cells in the gated thymic CD45<sup>-</sup>EpCAM<sup>+</sup> UEA-1<sup>+</sup> cells of WT and Wip1KO mice are summarized. (F) Total cell numbers of CD45<sup>-</sup>EpCAM<sup>+</sup> UEA-1<sup>+</sup> MHC II<sup>high</sup>, CD45<sup>-</sup>EpCAM<sup>+</sup> UEA-1<sup>+</sup> CD80<sup>+</sup>, CD45<sup>-</sup>EpCAM<sup>+</sup> UEA-1<sup>+</sup> CD40<sup>+</sup>, and CD45<sup>-</sup>EpCAM<sup>+</sup> UEA-1<sup>+</sup> Aire<sup>+</sup> cells in WT and Wip1KO mice are summarized. (G) The expression of Aire-dependent and -independent tissue-restricted Ags in sorted WT and Wip1KO mTECs were determined by real-time PCR. Data are representative of two to three independent experiments. Data presented are means ± SD (n = 5). \*p < 0.05, \*\*p < 0.01, \*\*\*p < 0.001 compared with WT controls. (H) H&E staining of WT and Wip1KO thymus is shown. The poor Hassall's corpuscle in Wip1KO thymus is noted (upper panel, original magnification ×20; lower panel, original magnification ×40). (I) Cell number of involucrin<sup>+</sup> UEA-1<sup>+</sup> cells in the thymi of WT and Wip1KO mice. Data presented are means ± SD (n = 5). \*\*\*p < 0.001 compared with WT mice.

ation of thymic epithelium in Wip1-deficient mice. The percentage of Foxp3<sup>+</sup>CD4<sup>+</sup>CD8<sup>-</sup> thymocytes, identified as a phenotype of natural regulatory T cells (32, 33), was significantly increased in the thymi of Wip1KO mice (p < 0.001, Fig. 3D). However, the total cell number of Foxp3<sup>+</sup>CD4<sup>+</sup>CD8<sup>-</sup> thymocytes in Wip1KO mice was similar to those found in WT mice (Fig. 3D). These data indicate that the development of Foxp3<sup>+</sup>CD4<sup>+</sup>CD8<sup>-</sup> natural regulatory T cells in Wip1KO thymus might not be impaired and the increased percentage of Foxp3<sup>+</sup>CD4<sup>+</sup>CD8<sup>-</sup> natural regulatory T cells in Wip1KO thymus was likely caused by the decreased Foxp3<sup>-</sup>CD4<sup>+</sup>CD8<sup>-</sup> thymocytes.

*Wip1 intrinsically regulates mTEC development*

Does Wip1 affect the EpCAM<sup>+</sup> UEA-1<sup>+</sup> mTEC population intrinsically? When we adoptively transferred WT or Wip1-deficient BMCs, respectively, into lethally irradiated syngeneic recipients to establish full hematopoietic chimeras, identical thymocyte numbers, percentages of CD45<sup>-</sup>EpCAM<sup>+</sup> TECs and EpCAM<sup>+</sup> UEA-1<sup>+</sup>

mTECs, and cell numbers of EpCAM<sup>+</sup> UEA-1<sup>+</sup> mTECs were observed in recipients receiving Wip1-deficient BMCs and those receiving WT BMCs (p > 0.05, Supplemental Fig. 1), indicating that Wip1 deficiency in hematopoietic-derived cells, such as thymocytes, B cells, and dendritic cells, does not significantly impact mTEC development. Reversely, Wip1-deficient mice grafted with WT BMCs showed smaller thymus size, decreased cell numbers of TECs, and decreased percentages of EpCAM<sup>+</sup> UEA-1<sup>+</sup> mTECs, MHC II<sup>high</sup> mTECs, CD40<sup>+</sup> mTECs, CD80<sup>+</sup> mTECs, and Aire<sup>+</sup> mTECs compared with WT mice reconstituted with WT BMCs (p < 0.001, Fig. 4A–G). Additionally, we grafted fetal Wip1KO and WT thymic lobes into T cell-deficient nude mice to further determine whether Wip1 intrinsically controls mTEC development. One to 2 mo after grafting, Wip1KO thymus grafts were significantly smaller than WT thymus grafts in nude mouse recipients (Fig. 4H, HI). The total cell numbers of CD45<sup>-</sup>EpCAM<sup>+</sup> TECs and EpCAM<sup>+</sup> UEA-1<sup>+</sup> mTECs were lower in Wip1KO thymus grafts than in WT thymus grafts (p < 0.05, Fig.

Table I. Sequencing primers used in the present study

Primers	Sense Sequence (5'→3')	Antisense Sequence (5'→3')
Aire	GGATGGAATGCTACGCCGTCTG	GGCAGCCTTCCTTCTCCTTCAG
spt1	TGGAAGTGCATGATTCGCTGGT	TGTTGTCAACGCCACTGTTCTG
Insulin1	CCATCAGCAAGCAGGTCATTTGT	CCAACGCCAAGGCTCTGAAGGT
Insulin2	GGAGGCTCTCTACCTGGTGTGT	TCTACAATGCCACGCTTCTGCT
Tff3	AATGCTGTTGGTGGTCTCGGTT	AGCAGCCACGGTTGTACACT
Mup1	TGGCCGAGAACCAGATTTGAGT	GAGGCAGCATCTGTAGTGTGA
nAchr-1	ACCTGGACCTATGACGGCTCTG	CGCTGCATGACGAAGTGGTAGG
GAD67	CTGCTCCAGTGTCTGCCATTC	CACGGTGCCCTTTGCTTTCCA
CRP	GCTACTCTGGTGCCTTCTGATC	AAGAGAAGACTGAAGCTGCG
RANK	ATGAGCATCTCGGACGGTGTG	GCCTTGCCCTGCATCACAGACTT
LTβR	GCACAGAAGCCGAGGTCACAGA	AGAGGACCAGCGACAGCAGGAT
Wnt4	CTCAAAGGCTGATCCAGAG	TCACAGCCACACTTCTCCAG
FGFR2IIIb	AGTCTGCCCTGGCTCACTGTCTT	AGCTGGCTGGCTGCTGAAGTCT
CD40	TGAGCCAAGACAGAGCCAGTG	CAGTGAACGCCGACGAAGA

4J). Meanwhile, the decreased percentages and cell numbers of EpCAM<sup>+</sup>UEA-1<sup>+</sup> mTECs and mature EpCAM<sup>+</sup>UEA-1<sup>+</sup> mTECs such as CD80<sup>+</sup>, Aire<sup>+</sup> cells in Wip1KO thymic grafts were detected ( $p < 0.05$ , Fig. 4K). Functionally, the cell numbers of thymocyte subsets, including CD4<sup>-</sup>CD8<sup>-</sup>, CD4<sup>+</sup>CD8<sup>+</sup>, CD4<sup>+</sup>CD8<sup>-</sup>, and CD4<sup>-</sup>CD8<sup>+</sup> cells in Wip1KO thymic grafts, were significantly lower than in WT thymic grafts ( $p < 0.001$ , Fig. 4L). Based on these data, we concluded that Wip1 is important for regulating the EpCAM<sup>+</sup>UEA-1<sup>+</sup> mTEC maturation compartment pool in an intrinsic manner.

#### Loss of Wip1 expression impacts adult thymic regeneration but not fetal mTEC development

To determine whether Wip1 is involved in thymic epithelium regeneration after thymus damage, we detected the recovery efficiency of TEC subsets in 8-wk-old Wip1KO and WT mice treated with Cy. Because Wip1KO mice had a smaller thymus than did WT mice before Cy treatment, we chose the recovery ratio of cell number as a parameter to determine the thymic regeneration ability in these assays. As shown in Fig. 5, by 14 d after Cy treatment, WT thymus weight and thymocyte subsets were recovered at 70–80%

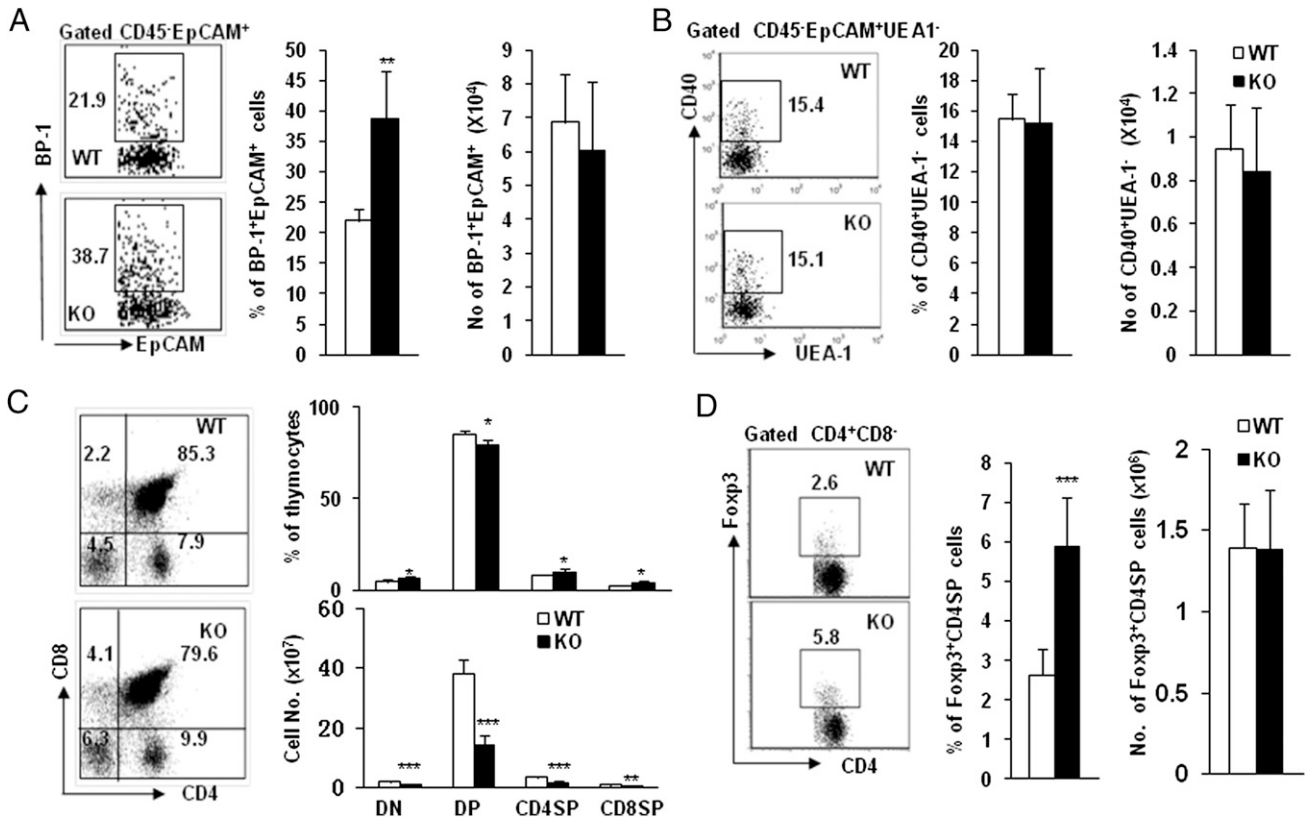


**FIGURE 3.** Normal cTEC subset and altered thymocyte subset development in Wip1KO mice were observed. **(A)** Representative FACS profiles of BP-1 molecule in the gated thymic CD45<sup>-</sup>EpCAM<sup>+</sup> cells as well as the percentage and cell number of CD45<sup>-</sup>EpCAM<sup>+</sup>BP-1<sup>+</sup> cells in WT and Wip1KO mice are shown. **(B)** Fractional abundance and total number of CD45<sup>-</sup>EpCAM<sup>+</sup>UEA-1<sup>-</sup>CD40<sup>+</sup> cells in WT and Wip1KO mice are shown. **(C)** Representative FACS staining of thymocytes as well as the percentage and cell number of each subset in WT and Wip1KO mice are presented. **(D)** Representative FACS intracellular staining of Foxp3 in the gated thymic CD4<sup>+</sup>CD8<sup>-</sup> thymocytes as well as the percentage and cell number of CD4<sup>+</sup>CD8<sup>-</sup>Foxp3<sup>+</sup> cells in WT and Wip1KO mice are shown. Data presented are the means  $\pm$  SD ( $n = 6$ ); one representative of three independent experiments with identical results is shown. \* $p < 0.05$ , \*\* $p < 0.01$ , \*\*\* $p < 0.001$  compared with WT controls.

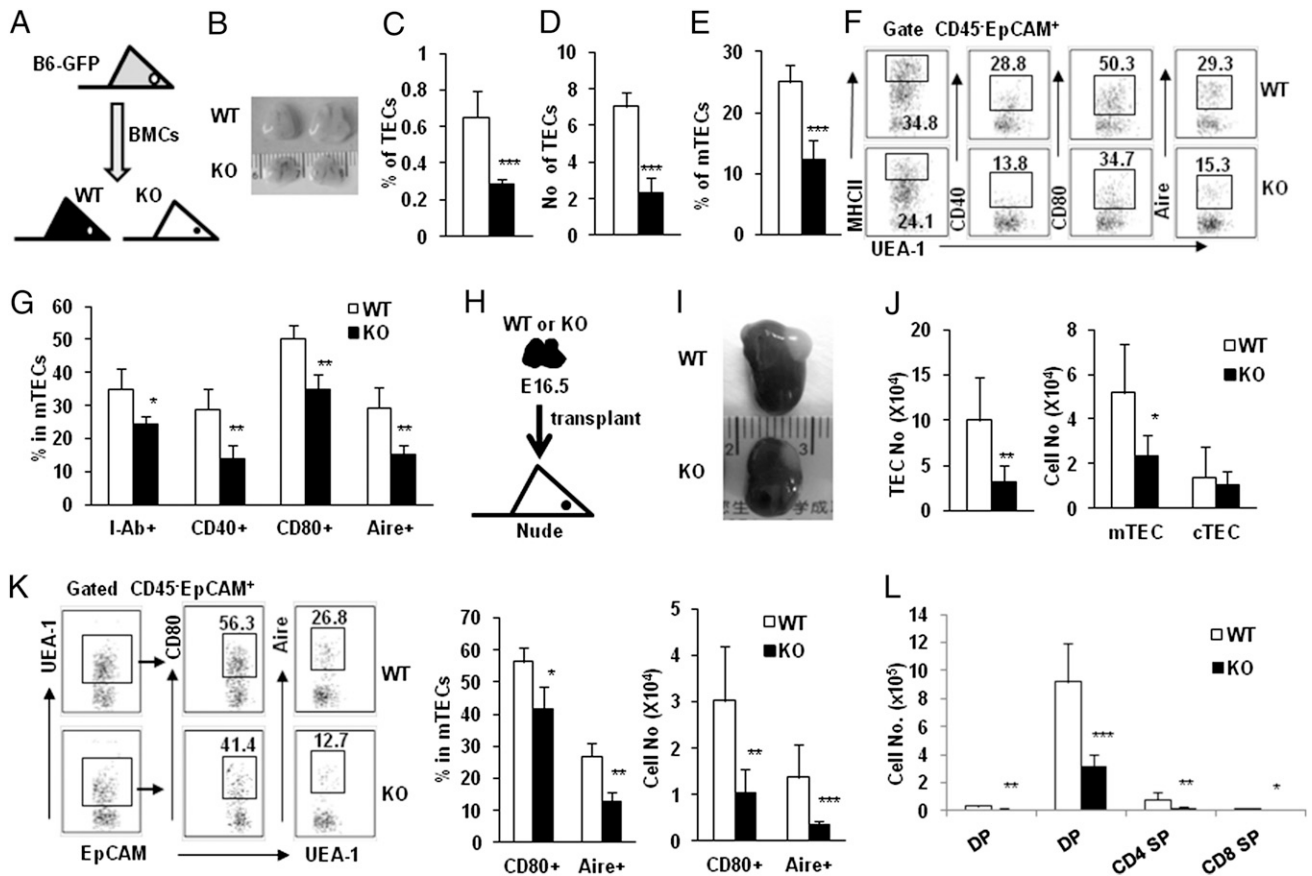


**FIGURE 4.** Wip1 deficiency impacts mTECs intrinsically. (A) Full chimeric mice were generated by transplanting B6-GFP WT BMCs to lethally irradiated WT or Wip1KO mice. By 12 wk after transplantation of WT BMCs, the TEC subsets were assayed. (B) Representative photographs of thymus organs in recipient WT and Wip1KO mice that received WT BMCs. The percentage of CD45<sup>+</sup>EpCAM<sup>+</sup> TEC cells (C), the total cell number of CD45<sup>+</sup>EpCAM<sup>+</sup> TEC cells (D), and the percentage of CD45<sup>+</sup>EpCAM<sup>+</sup>UEA-1<sup>+</sup> mTEC cells (E) in WT and Wip1KO mouse recipients of WT BMCs are shown. (F) Representative FACS staining of MHC II, CD40, CD80, and Aire expressions in the gated thymic CD45<sup>+</sup>EpCAM<sup>+</sup>UEA-1<sup>+</sup> cells of WT and Wip1KO mouse recipients is shown. (G) The total cell numbers of CD45<sup>+</sup>EpCAM<sup>+</sup>UEA-1<sup>+</sup>MHC II<sup>high</sup>, CD45<sup>+</sup>EpCAM<sup>+</sup>UEA-1<sup>+</sup>CD40<sup>+</sup>, CD45<sup>+</sup>EpCAM<sup>+</sup>UEA-1<sup>+</sup>CD80<sup>+</sup>, and CD45<sup>+</sup>EpCAM<sup>+</sup>UEA-1<sup>+</sup>Aire<sup>+</sup> cells in WT and Wip1KO mouse recipients are summarized. (H) Fetal WT and Wip1KO mouse thymi (16.5 d) were grafted into T cell-deficient BALB/c nude mice. By 6 wk after grafting, the thymic epithelial cells and thymocytes were studied. (I) Representative photographs of WT and Wip1KO thymic grafts. (J) The total cell numbers of CD45<sup>+</sup>EpCAM<sup>+</sup> TECs, CD45<sup>+</sup>EpCAM<sup>+</sup>UEA-1<sup>+</sup> mTECs, and CD45<sup>+</sup>EpCAM<sup>+</sup>BP-1<sup>+</sup> mTECs in thymic grafts are summarized. (K) The percentages and total cell numbers of CD45<sup>+</sup>EpCAM<sup>+</sup>UEA-1<sup>+</sup>CD80<sup>+</sup> and CD45<sup>+</sup>EpCAM<sup>+</sup>UEA-1<sup>+</sup>Aire<sup>+</sup> cells in WT and Wip1KO thymic grafts are summarized. (L) Cell numbers of thymocyte subsets in WT and Wip1KO thymic grafts are shown. Data (mean  $\pm$  SD,  $n = 5$ ) are from one of three independent experiments with similar results. \* $p < 0.05$ , \*\* $p < 0.01$ , \*\*\* $p < 0.001$  compared with WT group.

of normal levels, but Wip1KO mice were recovered at  $<50\%$  ( $p < 0.001$ , Fig. 5A–C). Meanwhile, the CD45<sup>+</sup>EpCAM<sup>+</sup> TECs including MHC II<sup>high</sup> and MHC II<sup>low</sup> subsets recovered 70% of normal levels in WT mice, but these cell populations reached only  $\sim 35\%$  in Wip1KO mice ( $p < 0.01$ , Fig. 5D, 5E). Whereas the recovery of cTECs was identical in WT and Wip1KO mice ( $p > 0.05$ , Fig. 5F), mTECs including relatively mature mTECs such as MHC II<sup>high</sup>, CD80<sup>+</sup>, CD40<sup>+</sup>, and Aire<sup>+</sup> cells were unable to be recovered efficiently in Wip1KO mice after Cy treatment ( $p < 0.01$ , Fig. 5G, 5H). These data suggested that Wip1 deficiency decreased the regenerative potentiality of mTECs after tissue damage.

The thymus originates from the third pharyngeal pouch endoderm during embryogenesis. Thymus organ development progresses from initial thymus cell fate specification through multiple stages of cTEC and mTEC differentiation (2). Does Wip1 deficiency impact thymus organogenesis and TEC development in the fetus? We studied the embryonic 16.5-d-old fetus and failed to detect any significant alteration of the fetal thymus with respect to thymus size, thymocyte number, as well as percentage and cell

number of mTECs and cTECs when analyzed by multicolor flow cytometry (Supplemental Fig. 2). Thus, Wip1 is unlikely involved in fetal thymus development, but it participates in postnatal homeostatic maintenance of the thymic medullary epithelium.

#### Wip1 deficiency decreases mTEC proliferation and differentiation kinetics

The mTEC defect of Wip1KO mice might be due to an increase of cell death and/or a decrease in the differentiation of mTECs from progenitors. To address the first possibility, we detected the cell death rate of TECs, mTECs, and cTECs as assayed by TUNEL staining. TECs in Wip1KO mice showed similar cell death kinetics as those of WT mice (Supplemental Fig. 3). Alternatively, the expression of apoptosis-related genes such Bcl-x<sub>L</sub>, Bcl-2, and Bax in TECs and mTECs was also identical in WT and Wip1KO mice (data not shown). Thus, it is unlikely that the decreased frequency and cell numbers of mTECs in the absence of Wip1 are due to the altered survival ability of mTECs.

It is speculated that the turnover time for mature CD80<sup>+</sup> mTECs in postnatal thymus is between 2 and 3 wk (34, 35). We next

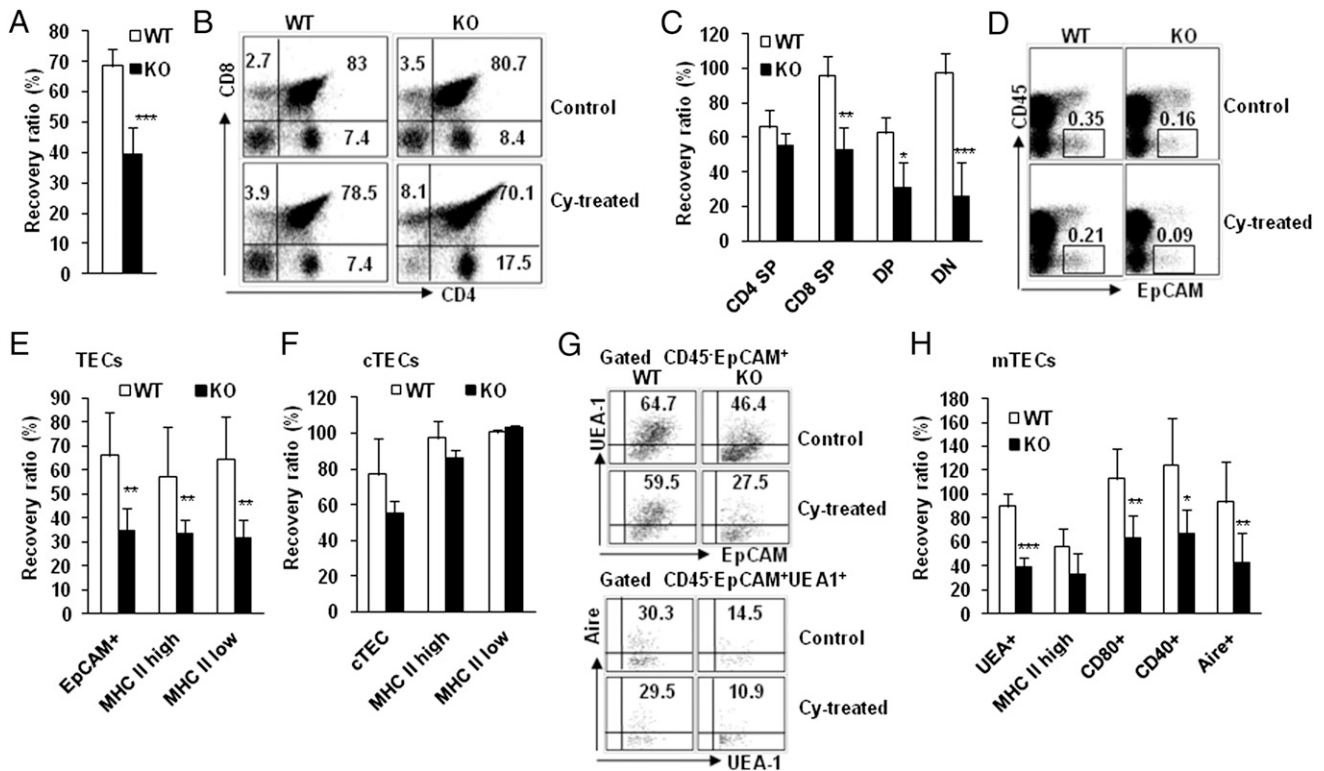


**FIGURE 5.** Delayed recovery of mature mTECs was observed in Wip1KO mice after Cy treatment. **(A)** The recovery ratio of thymocyte cell number in Wip1KO mice was lower than in WT mice after Cy treatment. **(B)** Flow cytometry analysis of CD4 and CD8 expressions in thymocytes of WT and Wip1KO mice treated with Cy or not is shown. **(C)** The delayed recovery of thymocyte subsets in Wip1KO mice was observed. **(D)** Representative FACS staining of thymic CD45<sup>+</sup>EpCAM<sup>+</sup> cells of WT and Wip1KO mice is shown. **(E)** The recovery ratio of CD45<sup>+</sup>EpCAM<sup>+</sup>, CD45<sup>+</sup>EpCAM<sup>+</sup>MHC II<sup>high</sup>, and CD45<sup>+</sup>EpCAM<sup>+</sup>MHC II<sup>low</sup> cells in Wip1KO mice were slower than in WT mice after Cy treatment. **(F)** The recovery ratios of CD45<sup>+</sup>EpCAM<sup>+</sup>BP-1<sup>+</sup>, CD45<sup>+</sup>EpCAM<sup>+</sup>BP-1<sup>+</sup>MHC II<sup>high</sup>, and CD45<sup>+</sup>EpCAM<sup>+</sup>BP-1<sup>+</sup>MHC II<sup>low</sup> cells in WT and Wip1KO mice after Cy treatment were identical. **(G)** Representative FACS profiles of MHC II, CD40, CD80, and Aire expressions in the gated thymic CD45<sup>+</sup>EpCAM<sup>+</sup>UEA-1<sup>+</sup> cells of WT and Wip1KO mice are shown. **(H)** The recovery of CD45<sup>+</sup>EpCAM<sup>+</sup>UEA-1<sup>+</sup>MHC II<sup>high</sup>, CD45<sup>+</sup>EpCAM<sup>+</sup>UEA-1<sup>+</sup>CD40<sup>+</sup>, CD45<sup>+</sup>EpCAM<sup>+</sup>UEA-1<sup>+</sup>CD80<sup>+</sup>, and CD45<sup>+</sup>EpCAM<sup>+</sup>UEA-1<sup>+</sup>Aire<sup>+</sup> cells in Wip1KO mice was slower than in WT mice after Cy treatment. Data are means  $\pm$  SD (four to seven mice per group) from one of two independent experiments. \* $p < 0.05$ , \*\* $p < 0.01$ , \*\*\* $p < 0.001$  (WT versus Wip1KO mice).

performed Ki67 expression and BrdU incorporation studies to examine the mTEC generation and homeostasis capacity. The percentage and absolute cell number of Ki67<sup>+</sup> cells were significantly lower in mTECs but not in TECs and cTECs of Wip1KO mice compared with the controls ( $p < 0.001$ , Fig. 6A, 6B). Similarly, by BrdU incorporation assay in vivo, the percentage and absolute cell number of BrdU<sup>+</sup> cells were significantly lower in mTECs but not in TECs and cTECs of Wip1KO mice compared with the controls ( $p < 0.01$ , Fig. 6C, 6D).

It was reported that bipotent progenitor cells for both mTECs and cTECs displayed an MTS24<sup>+</sup> phenotype (3, 4). To see whether Wip1 deficiency impacts thymic epithelial precursor/progenitor cells, we detected MTS24<sup>+</sup>EpCAM<sup>+</sup> cells in the thymus of Wip1KO and WT mice. Although the percentage of MTS24<sup>+</sup>EpCAM<sup>+</sup> cells was increased in Wip1KO mice ( $p < 0.001$ , Fig. 6E, 6F), the total cell number of MTS24<sup>+</sup>EpCAM<sup>+</sup> cells was identical in Wip1KO and WT mice ( $p > 0.05$ , Fig. 6G). We thus propose that Wip1 deficiency may mainly impair the differentiation process of MTS24<sup>+</sup>EpCAM<sup>+</sup> precursor cells into mTECs.

The upregulation of MHC II, CD80, and CD40 molecules and the transcriptional regulator Aire occur during UEA<sup>+</sup> mTEC differentiation and maturation (26–30). Expression levels were used to identify the developing stages of mTECs. Mature TECs express the highest levels of CD80 and Aire to be a CD80<sup>+</sup>Aire<sup>+</sup> phenotype (35, 36), although some controversy exists in this respect (30). Precursor-product analysis studies have shown that progenitors of MHC II<sup>high</sup>CD80<sup>+</sup>Aire<sup>+</sup> mTECs were contained within the

MHC II<sup>low</sup>CD80<sup>+</sup>Aire<sup>+</sup> mTEC subset (35, 36). The percentage of CD80<sup>+</sup>Aire<sup>+</sup> mature mTECs decreased whereas the percentage of CD80<sup>+</sup>Aire<sup>+</sup> immature mTECs increased in the fraction of UEA-1<sup>+</sup>EpCAM<sup>+</sup> mTECs in Wip1KO mice ( $p < 0.01$ , Fig. 6H, 6I). Importantly, the cell numbers of CD80<sup>+</sup>Aire<sup>+</sup> mature mTECs and CD80<sup>+</sup>Aire<sup>+</sup> intermediate mature mTECs were significantly decreased ( $p < 0.001$ , Fig. 6J) and the cell numbers of CD80<sup>+</sup>Aire<sup>+</sup> immature mTECs were slightly but significantly decreased in Wip1KO mice compared with WT mice (Fig. 6J). Thus, the ratio of CD80<sup>+</sup>Aire<sup>+</sup> mature mTECs to CD80<sup>+</sup>Aire<sup>+</sup> immature mTECs was markedly lower in Wip1KO mice than in WT mice (Fig. 6K), indicating the disrupted process kinetics of mTEC differentiation in Wip1KO mice. Therefore, these data collectively illustrate that decreased cell proliferation and/or maturation during progenitor cell differentiation into mature mTECs may contribute to poor medullary epithelial compartment of Wip1-deficient mice.

#### *Wip1 regulates mTEC differentiation through a p38 MAPK/CD40 signal pathway*

To date, three TNFRSF members, that is, RANK, CD40 and LT $\beta$ R, have been shown to play a crucial role in thymus medulla development. Mice deficient of RANK, CD40, and LT $\beta$ R, respectively, displayed absence or abnormality of mTECs (7, 36–38). Additionally, fibroblast growth factors (FGFs) and Wnt4 signaling could also boost thymopoiesis as well as promote differentiation by working on both thymocytes and TECs (39, 40). To identify the molecular mechanisms that mediate the function of Wip1 in

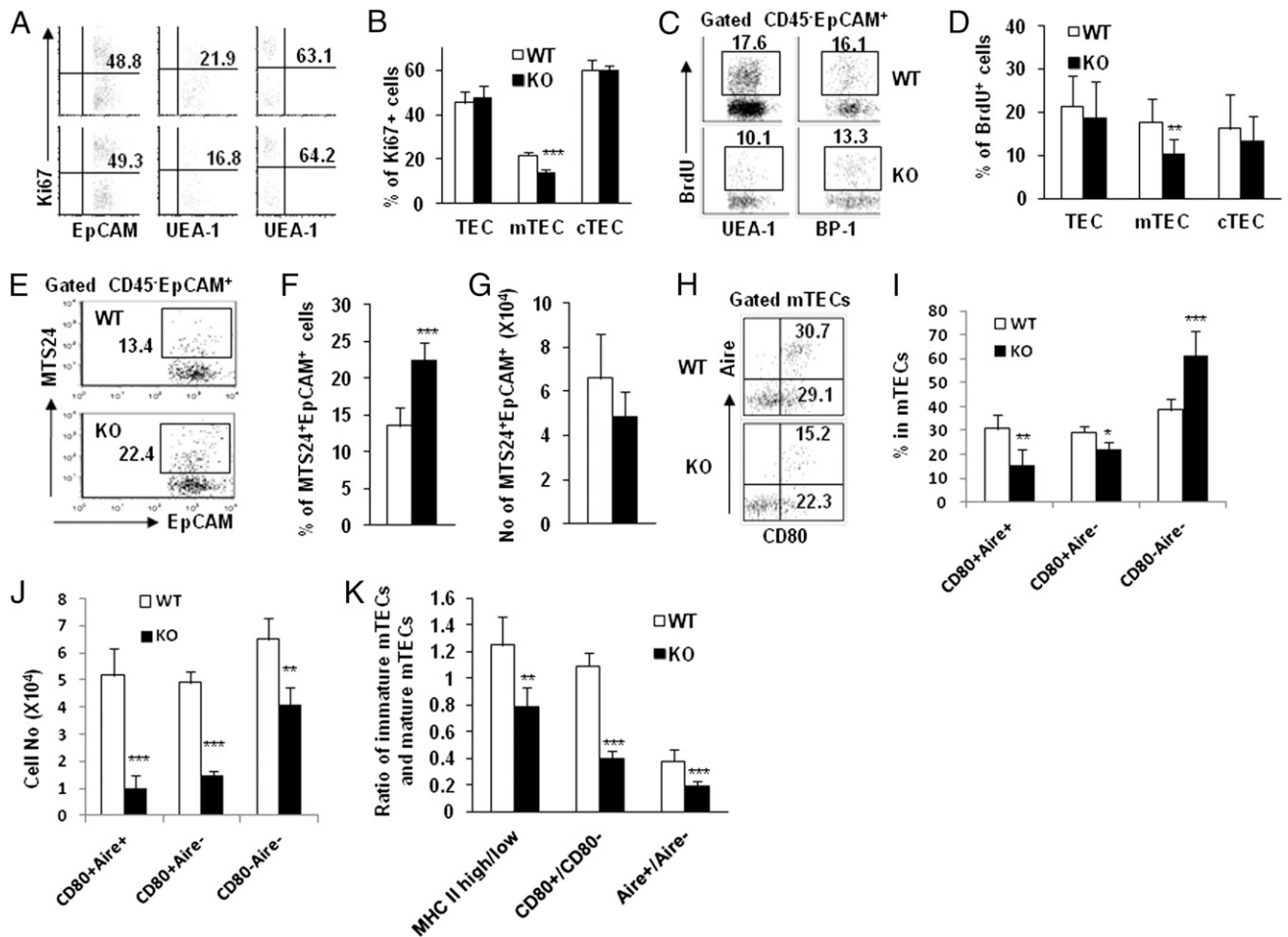


**FIGURE 6.** Decreased cell proliferation and differentiation kinetics of mTECs in Wip1KO mice were detected. **(A)** Representative FACS data for Ki67 staining in the gated thymic CD45<sup>-</sup>EpCAM<sup>+</sup> cells, CD45<sup>-</sup>EpCAM<sup>+</sup>UEA-1<sup>+</sup> cells, and CD45<sup>-</sup>EpCAM<sup>+</sup>UEA-1<sup>-</sup> cells of WT and Wip1KO mice are shown. **(B)** Percentages of CD45<sup>-</sup>EpCAM<sup>+</sup>UEA-1<sup>+</sup>Ki67<sup>+</sup> mTECs but not CD45<sup>-</sup>EpCAM<sup>+</sup>Ki67<sup>+</sup> TECs and CD45<sup>-</sup>EpCAM<sup>+</sup>UEA-1<sup>-</sup>Ki67<sup>+</sup> cTECs in Wip1KO mice decreased compared with those in WT mice. **(C)** Representative BrdU staining FACS analysis of CD45<sup>-</sup>EpCAM<sup>+</sup>UEA-1<sup>+</sup> cells and CD45<sup>-</sup>EpCAM<sup>+</sup>BP-1<sup>+</sup> cells in WT and Wip1KO mice 24 h after injection of BrdU. **(D)** A decreased percentage of CD45<sup>-</sup>EpCAM<sup>+</sup>UEA-1<sup>+</sup>BrdU<sup>+</sup> mTECs, but not CD45<sup>-</sup>EpCAM<sup>+</sup>BrdU<sup>+</sup> TECs, and CD45<sup>-</sup>EpCAM<sup>+</sup>UEA-1<sup>-</sup>BrdU<sup>+</sup> cTECs was observed in Wip1KO mice. Data are representative of four independent experiments. **(E)** FACS analysis of MTS24 expression in the gated thymic CD45<sup>-</sup>EpCAM<sup>+</sup> cells of WT and Wip1KO mice were shown. Increased percentage of EpCAM<sup>+</sup>MTS24<sup>+</sup> cells **(F)** but unchanged total cell number of EpCAM<sup>+</sup>MTS24<sup>+</sup> cells **(G)** was detected in Wip1KO mice. **(H)** CD80 and Aire molecules on the gated thymic CD45<sup>-</sup>EpCAM<sup>+</sup>UEA-1<sup>+</sup> mTECs of WT and Wip1KO mice were analyzed by FACS. **(I)** A decreased percentage of CD80<sup>+</sup>Aire<sup>+</sup> mature mTECs and an increased percentage of CD80<sup>-</sup>Aire<sup>-</sup> immature mTECs in Wip1KO mice were observed compared with WT mice. **(J)** Cell numbers of CD80<sup>+</sup>Aire<sup>+</sup> mature mTECs, CD80<sup>+</sup>Aire<sup>-</sup> intermedium mature mTECs, and CD80<sup>-</sup>Aire<sup>-</sup> immature mTECs in Wip1KO mice were compared with WT mice. **(K)** Decreased ratios of MHC II<sup>high</sup>/MHC II<sup>low</sup>, CD80<sup>+</sup>/CD80<sup>-</sup>, and Aire<sup>+</sup>/Aire<sup>-</sup> cells among CD45<sup>-</sup>EpCAM<sup>+</sup>UEA-1<sup>+</sup>mTECs in Wip1KO mice were observed compared with WT mice. Data represent the means  $\pm$  SD ( $n = 4$  mice/group) from one of four independent experiments. \*\* $p < 0.01$ , \*\*\* $p < 0.001$  (WT versus Wip1KO mice).

mTEC proliferation and differentiation, we examined the expression of TNFRSF members Wnt4 and FGF receptor (FGFR2IIIb) in Wip1KO mTECs by protein and mRNA levels. Wip1KO UEA-1<sup>+</sup> mTECs expressed similar levels of RANK and LT $\beta$ R as did WT cells as determined by FACS (Fig. 7A). Real-time PCR assays showed that the mRNA levels of RANK, LT $\beta$ R, Wnt4, and FGFR2IIIb in Wip1KO and WT mTECs were not significantly different (Fig. 7B). Consistent with decreased CD40 protein expression on mTECs as described above (Fig. 2), the CD40 mRNA expression in sorted Wip1KO mTECs was significantly lower than in WT mTECs (Fig. 7B). Therefore, Wip1 may control mTEC development and differentiation by governing CD40 expression.

The molecular signaling pathways that regulate CD40 expression in mTECs, and even in macrophages, have not been well defined. To understand the molecular mechanisms that mediate Wip1 function in the differentiation of mTECs, we assessed the potential involvement of intracellular downstream pathways of

Wip1, including p38 MAPK and STAT1 (20), in regulating CD40 expression. The freshly isolated mTECs, but not cTECs, from Wip1KO mice expressed higher levels of p38 MAPK activity than that of WT mice ( $p < 0.001$ , Fig. 7C). Interestingly, in the in vitro TEC culture system, inhibition of p38 MAPK but not STAT1 increased CD40 expression on mTECs ( $p < 0.01$ , Fig. 7D). In the FTOC system, inhibition of p38 MAPK significantly increased the percentage of CD80<sup>+</sup>Aire<sup>+</sup> mTECs (Fig. 7E). Adding CD40L significantly enhanced the percentages and cell numbers of CD80<sup>+</sup>Aire<sup>+</sup> mTECs in WT thymi (Fig. 7F, 7G). However, CD40L failed to induce CD80<sup>+</sup>Aire<sup>+</sup> mTECs in Wip1KO thymi ( $p < 0.01$ , Fig. 7F, 7G). Addition of RANKL in the FTOC system induced more CD80<sup>+</sup>Aire<sup>+</sup> mTECs in WT and Wip1KO thymi without significant difference ( $p > 0.05$ , Fig. 7F, 7G). All of these data demonstrated that the CD40 signaling pathway was impaired in Wip1KO mice. Therefore, p38 MAPK inhibits CD40 expression on mTECs and Wip1 deficiency increases p38 MAPK activity to downregulate

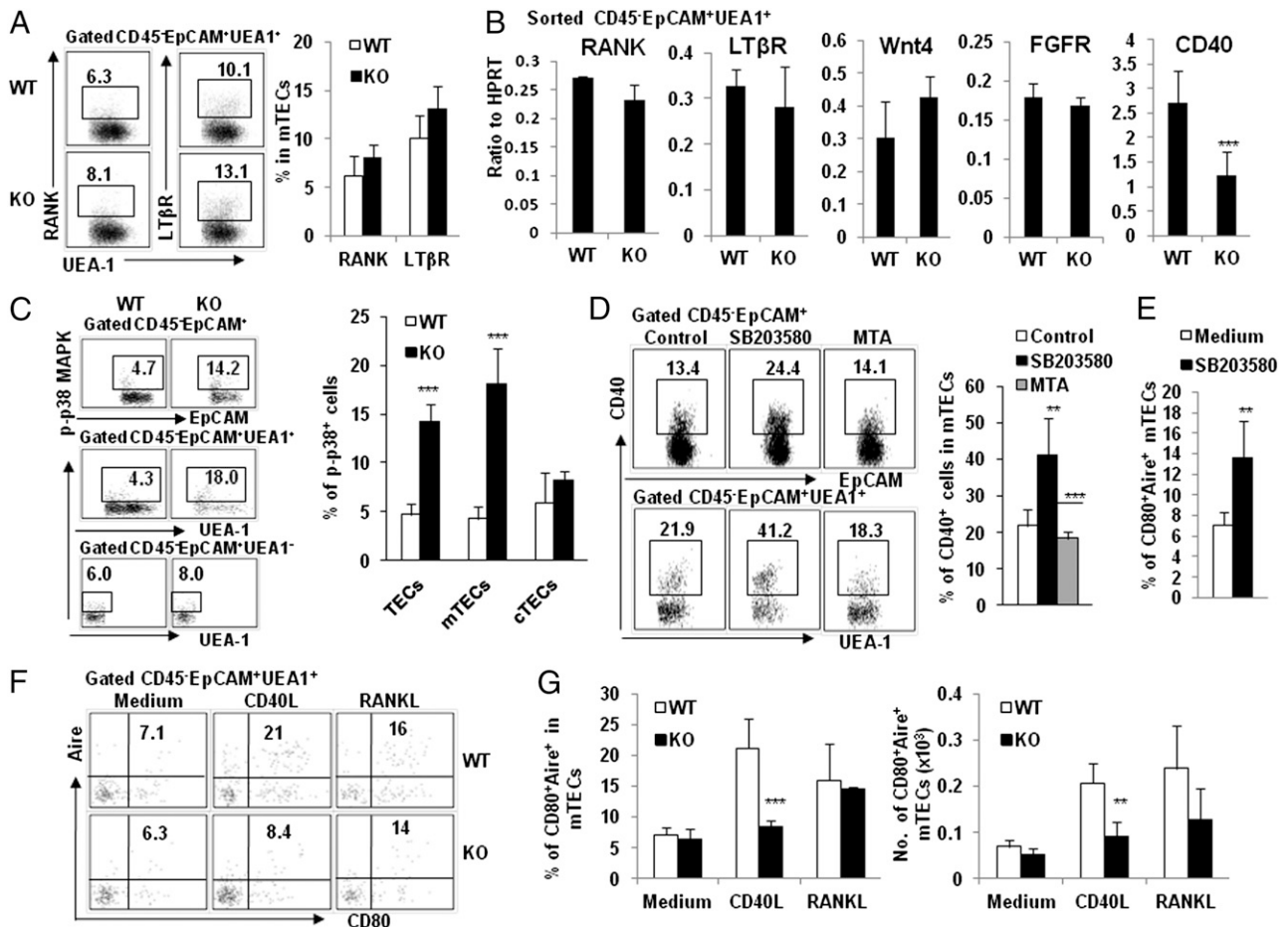


**FIGURE 7.** Wip1 deficiency decreased mTEC maturation by regulating CD40 signaling. **(A)** Flow cytometric analyses of RANK and LTβR expression on the gated CD45<sup>+</sup>EpCAM<sup>+</sup>UEA-1<sup>+</sup> mTECs of WT and Wip1KO mice are shown. **(B)** mRNA levels of RANK, LTβR, Wnt4, FGFR, and CD40 in sorted WT and Wip1KO mTECs were assayed by real-time PCR. **(C)** Representative FACS data and summary of p-p38 MAPK activity in Wip1KO TECs and mTECs compared with WT cells. **(D)** Primary TECs were cultured in vitro with PCT medium. Inhibiting p38 MAPK with 50 μM SB203580 but not STAT1 with 400 μM MTA for 48 h significantly increased CD40 expression on mTECs. **(E)** The percentages of CD80<sup>+</sup>Aire<sup>+</sup> mTECs in WT and Wip1KO thymus cultured with p38 MAPK inhibitor SB203580 in FTOC were summarized. **(F)** Flow cytometric analysis of CD80 and Aire expression on the gated CD45<sup>+</sup>EpCAM<sup>+</sup>UEA-1<sup>+</sup> mTECs of WT and Wip1KO thymus in FTOC cultured with CD40L and RANKL for 4 d is shown. **(G)** The percentage and cell number of CD80<sup>+</sup>Aire<sup>+</sup> mTECs of WT and Wip1KO thymus cultured with CD40L and RANKL are shown. Data presented are the means ± SD (*n* = 5 mice/group) from one of two independent experiments. \*\**p* < 0.01, \*\*\**p* < 0.001 between the indicated groups.

CD40 expression, which subsequently blocks mTEC differentiation and maturation.

## Discussion

In the present study, we provide evidence that Wip1 plays a key role in the control of mTEC development and maturation in both physical and pathological situations in an intrinsic manner. Wip1 deficiency in thymic epithelium selectively caused a severe defect of mTEC differentiation, as indicated by the decreased mTEC/cTEC ratio, medullary thymic zone, and the percentage and total cell number of mTECs in Wip1KO mice, WT bone marrow cell-transplanted Wip1KO mice, and fetal Wip1KO thymus-grafted mice. The significantly decreased mTECs including CD80<sup>+</sup>Aire<sup>+</sup> and involucrin<sup>+</sup>Aire<sup>+</sup> mTECs in unchallenged postnatal Wip1KO mice, as well as the poor mTEC recovery in Cy-treated adult Wip1KO mice, support that Wip1 not only controls mTEC turnover and homeostasis in physiological situation but also impacts mTEC regenerative ability in pathological conditions.

The lineage commitment and differentiation process and the relevant mechanisms for mTEC development are still poorly understood. Accumulated studies suggest that CD80<sup>+</sup>MHC II<sup>high</sup> or CD80<sup>+</sup>Aire<sup>+</sup> mature mTECs are derived from CD80<sup>-</sup>MHC II<sup>low</sup>

or CD80<sup>-</sup>Aire<sup>-</sup> immature mTECs (36). The decreased mTEC lineage differentiation in Wip1-deficient mice is likely to be the key reason for reduced thymic medullary region in these mice, as supported by the following evidence. First, Wip1KO mice had a normal thymic epithelial precursor MTS24<sup>+</sup> cell pool and unimpaired early developing mTECs such as CD80<sup>-</sup>Aire<sup>-</sup> cells, indicating that Wip1 is not involved in the early stages of mTECs. The ratio of mature-to-immature mTECs (CD80<sup>+</sup>Aire<sup>+</sup>/CD80<sup>-</sup>Aire<sup>-</sup> mTECs) in Wip1KO mice was significantly decreased, indicating that Wip1 controls mTEC developmental kinetics during mTEC maturation. Second, the lower BrdU incorporation into mTECs in Wip1KO mice indicates the decreased proliferation ability of developing mTEC in vivo. Third, Wip1KO mTECs showed an identical cell death ratio as control mice, as determined by TUNEL staining, excluding the possibility that Wip1 may affect the life span of mature mTECs. We conclude that Wip1 positively modulates the mTEC differentiation process and maturation state from its progenitor MTS24<sup>+</sup> cells.

The molecular networks regulating mTEC differentiation are still poorly defined. It has been reported that TNFRSFs, such as RANK, CD40, and LTβR, are important for mTEC maturation (7, 36), and deficiency in their downstream signaling regulator NF-κB

also causes thymus abnormality (8). Additionally, FGFs and Wnt4 could boost thymopoiesis as well as promote differentiation of TECs (39, 40). Wip1KO UEA-1<sup>+</sup> mTECs expressed similar levels of RANK, LT $\beta$ R, Wnt4, and FGFR2IIIb as WT cells as determined by FACS and real-time PCR assays. However, CD40 expression in Wip1KO mTECs was significantly lower than in WT mTECs. Therefore, Wip1 may regulate CD40 expression on mTECs to control mTEC development. A recent study has shown that CD40L/CD40 signaling controlled proliferation, but not the rate of apoptosis, within the mTEC compartment (41). These findings are consistent with our results in that Wip1 deficiency caused decreased proliferation but not apoptosis in mTECs.

To identify the molecular mechanisms that mediate the function of Wip1 in mTEC differentiation, we examined signaling pathways potentially activated by Wip1 in mTECs. We found that Wip1 deficiency caused the enhanced activation of p38 MAPK in mTECs. Notably, inhibiting p38 MAPK by SB203580, a specific pharmacological inhibitor of p38 $\alpha$  and p38 $\beta$  MAPK, remarkably enhanced CD40 expression on mTECs, indicating that Wip1 regulated mTEC differentiation via the p38 MAPK/CD40 pathway. Note that the defects of LT $\beta$ RKO, CD40KO, or TNFRSF11KO mouse lines in establishing the thymic medullary microenvironment appear to be substantially milder compared with TRAF6KO and RelBKO mice (7, 38). Thus, the decreased CD40 expression caused by Wip1 deficiency may be one of the altered pathways relevant to the severe defects of mTECs in Wip1KO mice. Other molecular pathways involved in the impaired mTEC development and maturation in Wip1KO mice should also be explored in the future. It was demonstrated that the activity of p53, which plays a central role in preserving genomic integrity, is one of the key target molecules attenuated by Wip1 in many different type of cells (42, 43). However, our preliminary study failed to detect the alteration of p53 activity in mTECs of Wip1-deficient mice. It was reported that the positive regulating role of Wip1 in T cell development in the thymus is dependent on the presence of p53 and its oncogenic activity (12, 18). The potential involvement of p53 in mTECs needs to be determined in the future.

Identical numbers and phenotypes of TECs were observed in the thymus of 16.5-d-old WT and Wip1KO fetus. Thus, Wip1 may not be involved in regulating mTEC development at the fetal stage. The different roles of Wip1 on mTEC maturation and homeostasis in fetal and postnatal stages may be explained by the distinct CD40 expression in these stages (41). The expression of CD40L was not detected in the fetal thymus but only began in the neonatal mice and predominantly in the medulla (44, 45), whereas CD40 was expressed in the TECs of fetal and neonatal thymi. This expression pattern supported the idea that the contribution of the CD40L/CD40 interaction to mTEC development might be limited before birth. Because Wip1 controlling mTEC development occurs via the CD40 pathway, it is not surprising that Wip1 regulates mTEC development after birth.

In summary, our data support a model in which Wip1 acts as a key regulator of the development, maturation, homeostasis, and function of mTECs under steady-state and "stressful" situations in adult mice but not in fetal mice. Mechanistic studies showed that Wip1 regulates mTEC maturation and homeostasis through the p38 MAPK/CD40 pathway. Wip1, as the phosphatase identified to be an intrinsic positive master for TECs, may be a promising target for therapeutic intervention to modulate mTEC function.

## Acknowledgments

We thank Dr. Xian C. Li and Douglas Corley for their review and editing of the manuscript; Prof. Richard Boyd (Monash University) for offering anti-MTS24 Ab; Prof. Francois-Xavier Hubert (Walter and Eliza Hall Institute

of Medical Research) for offering anti-Aire-FITC mAb; Tong Zhao, Jing Wang, Qing Meng, and Xiaoqi Liu for expert technical assistance; Qinghuan Li for excellent laboratory management; and Baisheng Ren for outstanding animal husbandry.

## Disclosures

The authors have no financial conflicts of interest.

## References

- Anderson, G., and Y. Takahama. 2012. Thymic epithelial cells: working class heroes for T cell development and repertoire selection. *Trends Immunol.* 33: 256–263.
- Manley, N. R., and B. G. Condie. 2010. Transcriptional regulation of thymus organogenesis and thymic epithelial cell differentiation. *Prog. Mol. Biol. Transl. Sci.* 92: 103–120.
- Bleul, C. C., T. Corbeaux, A. Reuter, P. Fisch, J. S. Mönning, and T. Boehm. 2006. Formation of a functional thymus initiated by a postnatal epithelial progenitor cell. *Nature* 441: 992–996.
- Rossi, S. W., W. E. Jenkinson, G. Anderson, and E. J. Jenkinson. 2006. Clonal analysis reveals a common progenitor for thymic cortical and medullary epithelium. *Nature* 441: 988–991.
- Blackburn, C. C., C. L. Augustine, R. Li, R. P. Harvey, M. A. Malin, R. L. Boyd, J. F. Miller, and G. Morahan. 1996. The nu gene acts cell-autonomously and is required for differentiation of thymic epithelial progenitors. *Proc. Natl. Acad. Sci. USA* 93: 5742–5746.
- Sun, L., H. Luo, H. Li, and Y. Zhao. 2013. Thymic epithelial cell development and differentiation: cellular and molecular regulation. *Protein Cell* 4: 342–355.
- Akiyama, T., Y. Shimo, H. Yanai, J. Qin, D. Ohshima, Y. Maruyama, Y. Asami, J. Kitazawa, H. Takayanagi, J. M. Penninger, et al. 2008. The tumor necrosis factor family receptors RANK and CD40 cooperatively establish the thymic medullary microenvironment and self-tolerance. *Immunity* 29: 423–437.
- Alexandropoulos, K., and N. M. Danzl. 2012. Thymic epithelial cells: antigen presenting cells that regulate T cell repertoire and tolerance development. *Immunol. Res.* 54: 177–190.
- Roberts, N. A., A. J. White, W. E. Jenkinson, G. Turchinovich, K. Nakamura, D. R. Withers, F. M. McConnell, G. E. Desanti, C. Benezech, S. M. Parnell, et al. 2012. Rank signaling links the development of invariant  $\gamma\delta$  T cell progenitors and Aire<sup>+</sup> medullary epithelium. *Immunity* 36: 427–437.
- Martins, V. C., T. Boehm, and C. C. Bleul. 2008. Lt $\beta$  signaling does not regulate Aire-dependent transcripts in medullary thymic epithelial cells. *J. Immunol.* 181: 400–407.
- Fiscella, M., H. Zhang, S. Fan, K. Sakaguchi, S. Shen, W. E. Mercer, G. F. Vande Woude, P. M. O'Connor, and E. Appella. 1997. Wip1, a novel human protein phosphatase that is induced in response to ionizing radiation in a p53-dependent manner. *Proc. Natl. Acad. Sci. USA* 94: 6048–6053.
- Le Guezennec, X., and D. V. Bulavin. 2010. WIP1 phosphatase at the crossroads of cancer and aging. *Trends Biochem. Sci.* 35: 109–114.
- Salminen, A., and K. Kaarniranta. 2011. Control of p53 and NF- $\kappa$ B signaling by WIP1 and MIF: role in cellular senescence and organismal aging. *Cell. Signal.* 23: 747–752.
- Lu, X., T. A. Nguyen, S. H. Moon, Y. Darlington, M. Sommer, and L. A. Donehower. 2008. The type 2C phosphatase Wip1: an oncogenic regulator of tumor suppressor and DNA damage response pathways. *Cancer Metastasis Rev.* 27: 123–135.
- Chew, J., S. Biswas, S. Shreeram, M. Humaidi, E. T. Wong, M. K. Dhillon, H. Teo, A. Hazra, C. C. Fang, E. López-Collazo, et al. 2009. WIP1 phosphatase is a negative regulator of NF- $\kappa$ B signalling. *Nat. Cell Biol.* 11: 659–666.
- Bulavin, D. V., C. Phillips, B. Nannenga, O. Timofeev, L. A. Donehower, C. W. Anderson, E. Appella, and A. J. Fornace, Jr. 2004. Inactivation of the Wip1 phosphatase inhibits mammary tumorigenesis through p38 MAPK-mediated activation of the p16<sup>Ink4a</sup>-p19<sup>Arf</sup> pathway. *Nat. Genet.* 36: 343–350.
- Oliva-Trastoy, M., V. Berthonaud, A. Chevalier, C. Ducrot, M. C. Marsolier-Kergoat, C. Mann, and F. Leteurtre. 2007. The Wip1 phosphatase (PPM1D) antagonizes activation of the Chk2 tumour suppressor kinase. *Oncogene* 26: 1449–1458.
- Schito, M. L., O. N. Demidov, S. Saito, J. D. Ashwell, and E. Appella. 2006. Wip1 phosphatase-deficient mice exhibit defective T cell maturation due to sustained p53 activation. *J. Immunol.* 176: 4818–4825.
- Choi, J., B. Nannenga, O. N. Demidov, D. V. Bulavin, A. Cooney, C. Brayton, Y. Zhang, I. N. Mbowu, A. Bradley, E. Appella, and L. A. Donehower. 2002. Mice deficient for the wild-type p53-induced phosphatase gene (Wip1) exhibit defects in reproductive organs, immune function, and cell cycle control. *Mol. Cell. Biol.* 22: 1094–1105.
- Liu, G., X. Hu, B. Sun, T. Yang, J. Shi, L. Zhang, and Y. Zhao. 2013. Phosphatase Wip1 negatively regulates neutrophil development through p38 MAPK-STAT1. *Blood* 121: 519–529.
- Gray, D. H., A. L. Fletcher, M. Hammett, N. Seach, T. Ueno, L. F. Young, J. Barbuto, R. L. Boyd, and A. P. Chidgey. 2008. Unbiased analysis, enrichment and purification of thymic stromal cells. *J. Immunol. Methods* 329: 56–66.
- Liu, G., S. Burns, G. Huang, K. Boyd, R. L. Proia, R. A. Flavell, and H. Chi. 2009. The receptor SIP1 overrides regulatory T cell-mediated immune suppression through Akt-mTOR. *Nat. Immunol.* 10: 769–777.
- Liu, G., K. Duan, H. Ma, Z. Niu, J. Peng, and Y. Zhao. 2011. An instructive role of donor macrophages in mixed chimeras in the induction of recipient CD4<sup>+</sup> Foxp3<sup>+</sup> Treg cells. *Immunol. Cell Biol.* 89: 827–835.

24. Duan, K., B. Zhang, W. Zhang, Y. Zhao, Y. Qu, C. Sun, and Y. Zhao. 2011. Efficient peripheral construction of functional human regulatory CD4<sup>+</sup>CD25<sup>high</sup> Foxp3<sup>+</sup> T cells in NOD/SCID mice grafted with fetal human thymus/liver tissues and CD34<sup>+</sup> cells. *Transpl. Immunol.* 25: 173–179.
25. Farr, A. G., and S. K. Anderson. 1985. Epithelial heterogeneity in the murine thymus: fucose-specific lectins bind medullary epithelial cells. *J. Immunol.* 134: 2971–2977.
26. Tykocinski, L. O., A. Sinemus, and B. Kyewski. 2008. The thymus medulla slowly yields its secrets. *Ann. N. Y. Acad. Sci.* 1143: 105–122.
27. Zhang, L., L. Sun, and Y. Zhao. 2007. Thymic epithelial progenitor cells and thymus regeneration: an update. *Cell Res.* 17: 50–55.
28. Gillard, G. O., and A. G. Farr. 2006. Features of medullary thymic epithelium implicate postnatal development in maintaining epithelial heterogeneity and tissue-restricted antigen expression. *J. Immunol.* 176: 5815–5824.
29. Galy, A. H., and H. Spits. 1992. CD40 is functionally expressed on human thymic epithelial cells. *J. Immunol.* 149: 775–782.
30. Nishikawa, Y., F. Hirota, M. Yano, H. Kitajima, J. Miyazaki, H. Kawamoto, Y. Mouri, and M. Matsumoto. 2010. Biphasic Aire expression in early embryos and in medullary thymic epithelial cells before end-stage terminal differentiation. *J. Exp. Med.* 207: 963–971.
31. Yano, M., N. Kuroda, H. Han, M. Meguro-Horike, Y. Nishikawa, H. Kiyonari, K. Maemura, Y. Yanagawa, K. Obata, S. Takahashi, et al. 2008. Aire controls the differentiation program of thymic epithelial cells in the medulla for the establishment of self-tolerance. *J. Exp. Med.* 205: 2827–2838.
32. Yi, H., Y. Zhen, L. Jiang, J. Zheng, and Y. Zhao. 2006. The phenotypic characterization of naturally occurring regulatory CD4<sup>+</sup>CD25<sup>+</sup> T cells. *Cell. Mol. Immunol.* 3: 189–195.
33. Zheng, Q., Y. Xu, Y. Liu, B. Zhang, X. Li, F. Guo, and Y. Zhao. 2009. Induction of Foxp3 demethylation increases regulatory CD4<sup>+</sup>CD25<sup>+</sup> T cells and prevents the occurrence of diabetes in mice. *J. Mol. Med.* 87: 1191–1205.
34. Gray, D. H., N. Seach, T. Ueno, M. K. Milton, A. Liston, A. M. Lew, C. C. Goodnow, and R. L. Boyd. 2006. Developmental kinetics, turnover, and stimulatory capacity of thymic epithelial cells. *Blood* 108: 3777–3785.
35. Gäbler, J., J. Arnold, and B. Kyewski. 2007. Promiscuous gene expression and the developmental dynamics of medullary thymic epithelial cells. *Eur. J. Immunol.* 37: 3363–3372.
36. Rossi, S. W., M. Y. Kim, A. Leibbrandt, S. M. Parnell, W. E. Jenkinson, S. H. Glanville, F. M. McConnell, H. S. Scott, J. M. Penninger, E. J. Jenkinson, et al. 2007. RANK signals from CD4<sup>+</sup>3<sup>-</sup> inducer cells regulate development of Aire-expressing epithelial cells in the thymic medulla. *J. Exp. Med.* 204: 1267–1272.
37. Hikosaka, Y., T. Nitta, I. Ohigashi, K. Yano, N. Ishimaru, Y. Hayashi, M. Matsumoto, K. Matsuo, J. M. Penninger, H. Takayanagi, et al. 2008. The cytokine RANKL produced by positively selected thymocytes fosters medullary thymic epithelial cells that express autoimmune regulator. *Immunity* 29: 438–450.
38. Boehm, T., S. Scheu, K. Pfeffer, and C. C. Bleul. 2003. Thymic medullary epithelial cell differentiation, thymocyte emigration, and the control of autoimmunity require lympho-epithelial cross talk via LTβR. *J. Exp. Med.* 198: 757–769.
39. Revest, J. M., R. K. Suniara, K. Kerr, J. J. Owen, and C. Dickson. 2001. Development of the thymus requires signaling through the fibroblast growth factor receptor R2-IIIb. *J. Immunol.* 167: 1954–1961.
40. Heinonen, K. M., J. R. Vanegas, S. Brochu, J. Shan, S. J. Vainio, and C. Perreault. 2011. Wnt4 regulates thymic cellularity through the expansion of thymic epithelial cells and early thymic progenitors. *Blood* 118: 5163–5173.
41. Desanti, G. E., J. E. Cowan, S. Baik, S. M. Parnell, A. J. White, J. M. Penninger, P. J. Lane, E. J. Jenkinson, W. E. Jenkinson, and G. Anderson. 2012. Developmentally regulated availability of RANKL and CD40 ligand reveals distinct mechanisms of fetal and adult cross-talk in the thymus medulla. *J. Immunol.* 189: 5519–5526.
42. Takekawa, M., M. Adachi, A. Nakahata, I. Nakayama, F. Itoh, H. Tsukuda, Y. Taya, and K. Imai. 2000. p53-Inducible Wip1 phosphatase mediates a negative feedback regulation of p38 MAPK-p53 signaling in response to UV radiation. *EMBO J.* 19: 6517–6526.
43. Lu, X., O. Ma, T. A. Nguyen, S. N. Jones, M. Oren, and L. A. Donehower. 2007. The Wip1 phosphatase acts as a gatekeeper in the p53-Mdm2 autoregulatory loop. *Cancer Cell* 12: 342–354.
44. Akiyama, T., S. Maeda, S. Yamane, K. Ogino, M. Kasai, F. Kajiura, M. Matsumoto, and J. Inoue. 2005. Dependence of self-tolerance on TRAF6-directed development of thymic stroma. *Science* 308: 248–251.
45. Dunn, R. J., C. J. Lueddeker, H. S. Haugen, C. H. Clegg, and A. G. Farr. 1997. Thymic overexpression of CD40 ligand disrupts normal thymic epithelial organization. *J. Histochem. Cytochem.* 45: 129–141.